Supplement of Biogeosciences, 17, 3631–3642, 2020
https://doi.org/10.5194/bg-17-3631-2020-supplement

Supplement of

Contrasting decadal trends of subsurface excess nitrate in the western and eastern North Atlantic Ocean

Jin-Yu Terence Yang et al.

Correspondence to: Kitack Lee (ktl@postech.ac.kr)

Text S1

Our analysis of NAtl nutrient data was primarily focused on data obtained during the past 3 decades. Previous studies have also confirmed that during this period the physical (i.e., potential temperature and salinity) and chemical (i.e., nutrients and oxygen) properties of deep waters (> 2000 m depth) in the western and eastern subtropical NAtl have not changed discernibly (Zhang et al., 2000; Gebbie and Huybers, 2012; Key et al., 2015; Olsen et al., 2016; Woosley et al., 2016). Moreover, we found no significant changes in salinity, potential temperature, and concentration of dissolved oxygen (DO) in the deep waters at the Bermuda Atlantic Time-series Study (BATS at 2000–3500 m depth) site in the western NAtl and at the Iceland Sea Time-series site (68.0°N, 12.7°W; at 1500–1800 m depth) in the eastern NAtl during the period 1990–2015 (Fig. S2).

The methods of nutrient and oxygen measurement in oceanography have been improved over time. The GO-SHIP program is an ongoing international repeat hydrography program and has provided the accurate oceanographic measurements using the most updated methodology (Talley et al., 2016). On each of the four transects the concentration profiles of nutrients and DO measured during the most recent cruises (the GO-SHIP program; Table S1) were used as the reference to correct the inaccuracy in historical data because of limitations in analytical technique and instrumentation used in early days. The differences (individual cruise data minus the GO-SHIP data) in concentrations of DIN, DIP, and DO in deep waters (where the concentration gradients were smallest) within a pixel of 1° (or 1.5°) latitude by 1.5° longitude were then calculated (Fig. S1b). For each pixel the estimated differences for all parameters along the density layers were finally applied to all cruise data other than the reference GO-SHIP data collected from the same pixel (Fig. S3). This data adjustment method would minimize systematic errors in data used in our analysis (Zhang et al., 2000).

Changes in nutrient concentrations associated with changes in remineralization (equivalent to changes in apparent oxygen utilization; AOU) were corrected using the DIP:DIN:O_2 remineralization ratio of 1:15:(–160) (Anderson and Sarmiento, 1994). We found no discernable effect of remineralization on any of the NAtl deep water DIN_{xs} values, which is consistent with the results of previous studies (Broecker and Takahashi, 1980). For individual locations, multiplicative adjustment factors for nutrient concentrations were applied to the entire water column data if any differences were found in the deep waters (Key et al., 2015; Olsen et al., 2016).

Table S1. Detailed information of cruises and transects used in this study. Data collected in these cruises were shown in Figure 1.

Program/ Data source	Expocode	Date	Extent	Nominal Lat./Long.
		A22		
GEOSECS	GEOSECS_ATL	3/30/1973	35°N−36°N	67°W–68°W
TTO	316N19810401	4/5−4/25/1981	18.5°N−36°N	66°W
WOCE	316N19970815	8/15−9/3/1997	18.5°N−36°N	66°W
CLIVAR	316N20031023	10/23−11/13/2003	18.5°N−36°N	66°W
GO-SHIP	33AT20120324	3/24−4/17/2012	18.5°N−36°N	66°W
		A20		
GEOSECS	GEOSECS_ATL	9/20–9/28/1972	18°N−34°N	50°W−54°W
NODC	32OC19830501	5/1−5/17/1983	15°N−36°N	52°W
WOCE	316N19970717	7/17−8/10/1997	15°N−36°N	52°W
CLIVAR	316N20030922	9/22−10/23/2003	15°N−36°N	52°W
GO-SHIP	33AT20120419	4/19−5/1/2012	15°N−36°N	52°W
		A16N		
WOCE	32OC19880723	7/23−8/27/1988	20°N−64°N	20°W−25°W
CLIVAR	33RO20030604	6/4−8/1/2003	20°N−64°N	20°W−25°W
GO-SHIP	33RO20130803	8/13−9/9/2013	20°N−64°N	20°W−25°W
		A05		
WOCE	33RO19980123	1/23−2/24/1998	75°W−14°W	24.5°N
CLIVAR	74DI20040404	4/4−5/10/2004	75°W−14°W	24.5°N
GO-SHIP	74DI20100106	1/6−2/18/2010	75°W−14°W	24.5°N

Table S2. Overall average adjustment factors (%) obtained from comparisons of the nutrients (DIN and DIP) concentrations for the deep water along the four transects at crossover stations. The comparison data were taken from the depths with minimum concentration gradients. The latest GO-SHIP cruises (see Table S1) were used as the reference against which historical cruises were compared. The average adjustment factors for the DIN and DIP are consistent to those in the GLODAPv2 product (Olsen et al., 2016).

Transect/ Cruise year	Average adjustment factor (%)	
	DIN	DIP
A22		
1997	0.75±0.57	0.21±0.46
2003	−0.47±0.90	−1.54±0.60
A20		
1983	−0.39±1.01	−0.71±1.48
1997	–0.07±0.63	–0.44±0.57
2003	–0.17±0.76	–0.78±0.76
A16N		
1988	0.50±1.56	–4.03±3.00
2003	–0.02±1.60	–1.31±1.99
A05		
1998	0.14±1.68	1.05±1.79
2004	0.63±3.41	0.02±3.29

Table S3. Locations of monitoring sites of atmospheric wet nitrogen deposition along the US Atlantic coast. Annual average data of total inorganic nitrogen deposition were derived from the sites with an observation period were greater than 15 years. Data are available at http://nadp.sws.uiuc.edu/.

Site ID	Latitude (°N)	Longitude (°W)	Observational Period
FL03	29.9748	82.1978	1978–2016
FL05	28.7486	82.5551	1996–2016
FL11	25.3900	80.6800	1980–2016
FL41	27.3801	82.2831	1983–2016
FL99	28.5428	80.6440	1983–2015
GA09	30.7404	82.1283	1997–2016
GA20	32.0849	81.9367	1983–2016
MA01	41.9759	70.0241	1981–2016
ME96	43.8325	70.0645	1998–2016
ME98	44.3772	68.2608	1981–2016
NC03	36.1325	77.1708	1978–2016
NJ00	39.4728	74.4369	1998–2016
PR20	18.3206	65.8200	1985–2016

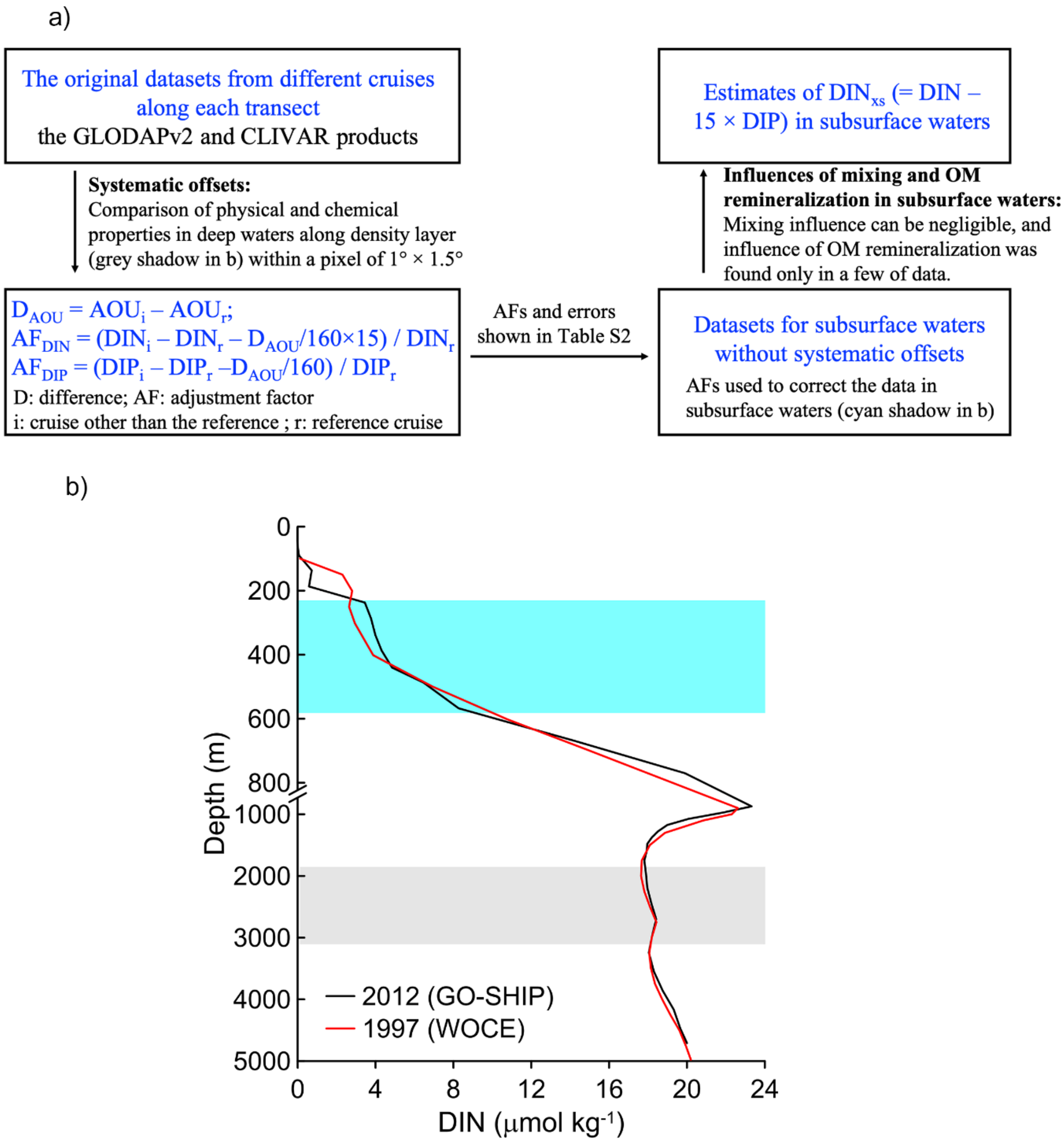

Figure S1. (a) Flow chart of the procedure used to adjust the original data from the GLODAPv2 product and CLIVAR database. (b) Example profile of DIN illustrating the adjustment methods. The main adjustments were derived from an examination of the systematic offsets that are shown in Table S2.

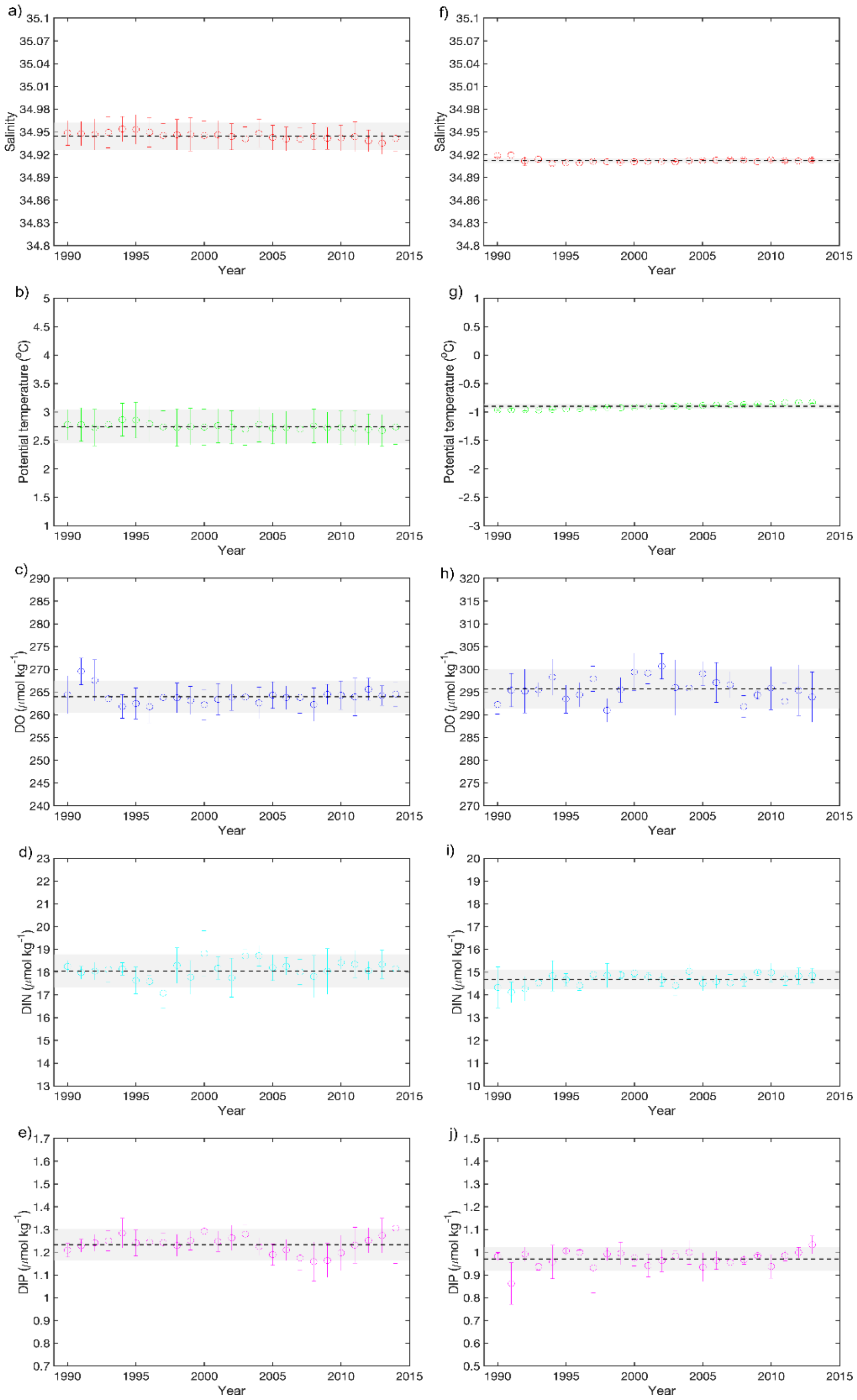

Figure S2. Temporal variations in salinity, potential temperature, and concentrations of dissolved oxygen (DO), DIN and DIP for the deep waters at the Bermuda Atlantic Time-series Study (BATS, 31.7°N, 64.2°W) site from 1990–2015 (a–e, 2000–3500 m) and a time-series site (68.0°N, 12.7°W) from 1990–2013 (f–j, 1500–1800 m) in the northern Iceland Sea. Data from BATS are derived from http://bats.bios.edu/bats-data/, while data from the Iceland Sea are from the Ocean Carbon Data System, NOAA (https://www.nodc.noaa.gov/ocads/oceans/Moorings/Iceland_Sea.html).

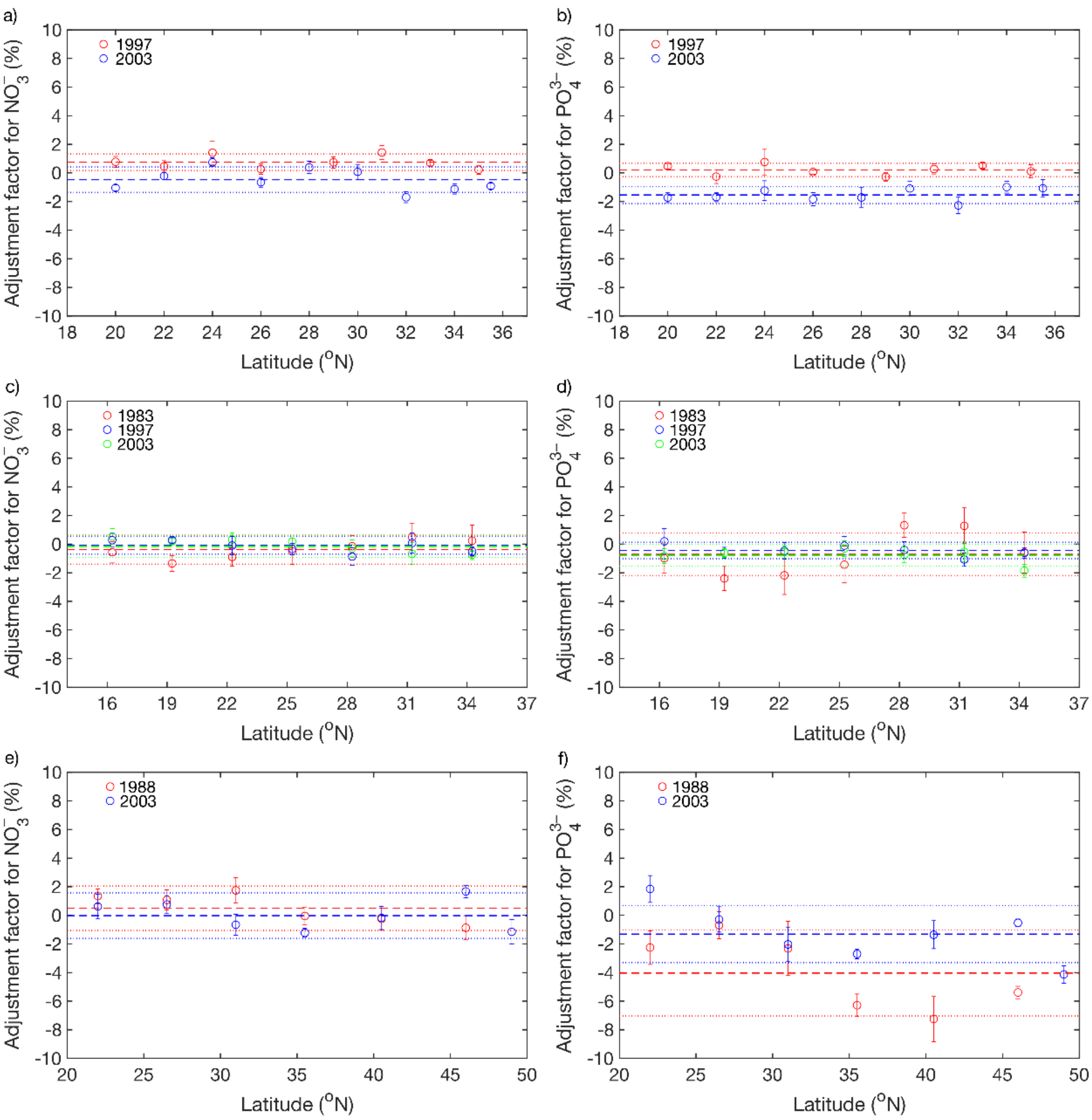

Figure S3. Adjustment factors of NO_3^- and PO_4^{3-} for the major cruises along A22 (a and b), A20 (c and d) and A16N (e and f) by 3°–5° latitude. Data from the latest GO-SHIP cruise along each transect were used as references. The adjustment factors were obtained by comparing the deep-water parameters of different cruises with the reference data. The relatively high adjustment factors obtained for A16N are a result of the use of raw data rather than data from the GLODAPv2 product, because the latest cruise along A16N in 2013 is not included in the GLODAPv2 product.

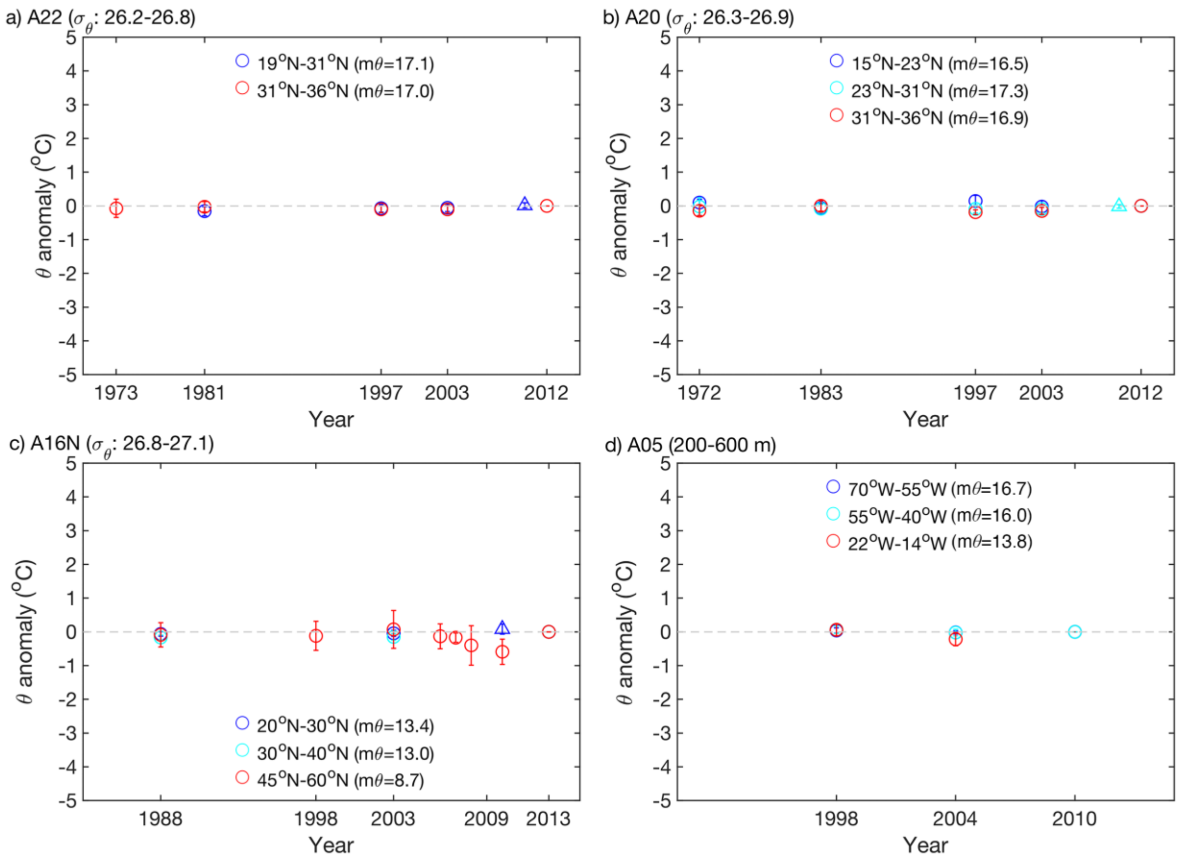

Figure S4. Temporal trends of potential temperature (θ) anomalies (dots) for the corresponding latitude or longitude intervals for the subsurface potential density intervals σ_θ along the four transects (a) A22, (b) A20, (c) A16N (note that σ_θ = 27.2–27.6 for the latitude interval of 45°N−60°N), and (d) A05 in the NAtl. The date from A05 obtained in 2010 at three crossover sites are also shown in a-c (triangles). θ anomalies indicate θ values minus the mean θ value in the GO-SHIP dataset (mθ, values shown in parentheses). The selected density intervals are typically located at a water depth of 200−600 m, which encompasses the DIN_{xs} maximum. The selected σ_θ intervals in the subpolar region along A16N and in the eastern basin along A05 were different, as σ_θ for 200−600 m depth becomes larger in the high-latitude region or eastern basin. The gray dashed line indicates a θ anomaly of zero. The θ of a water mass occupying any given density surface did not change between repeat occupations (Student's t-test and ANOVA with Games-Howell test, p > 0.05) along the four transects in the NAtl, except for a slight decrease in the subpolar region along A16N since the 2000s.

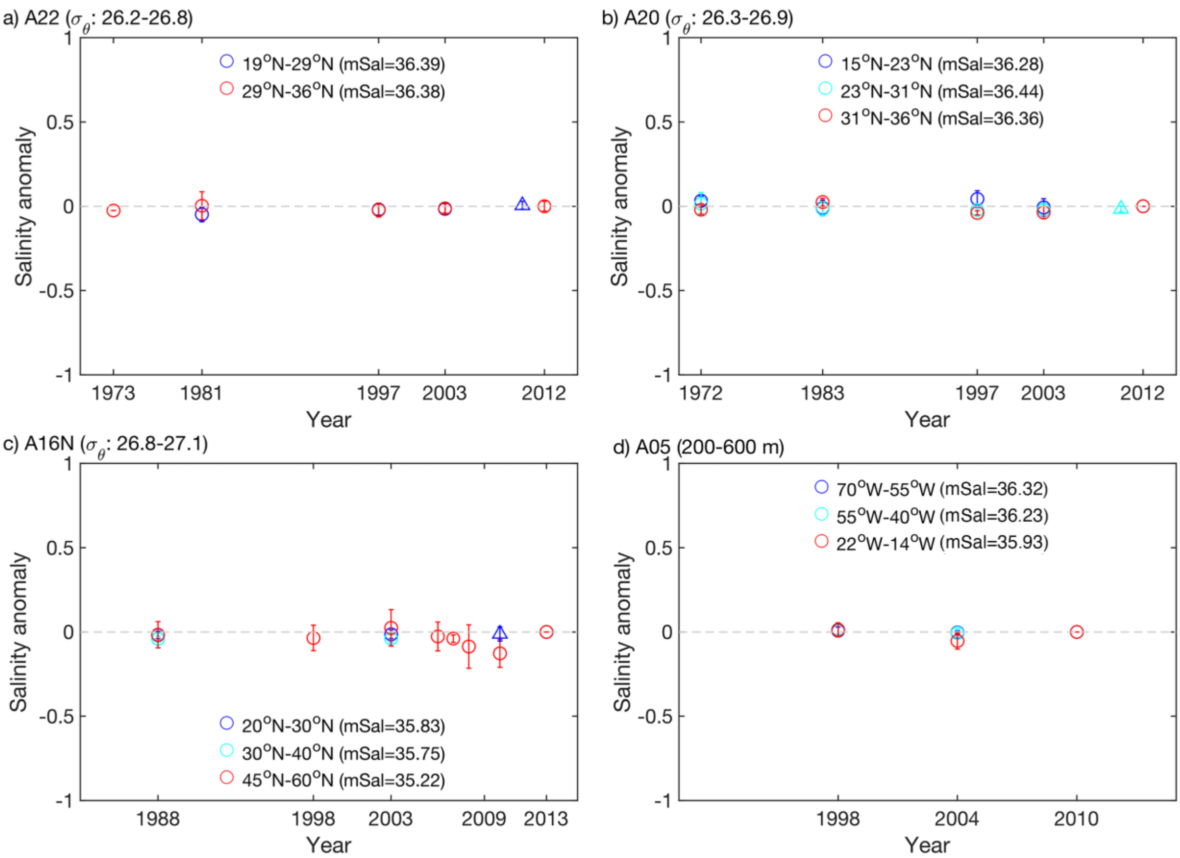

Figure S5. The same as in Figure S3 except for salinity anomalies. Salinity anomalies indicate salinity minus the mean value salinity in GO-SHIP dataset (mSal, their values in parentheses). The gray dashed lines indicate salinity anomaly of zero. The salinity of a water mass occupying any given density surface did not change between repeat occupations (Student's t-test and ANOVA with Games-Howell test, $p > 0.05$) along the four transects in the NAtl, except for a slight decrease in the subpolar region along A16N since the 2000s.

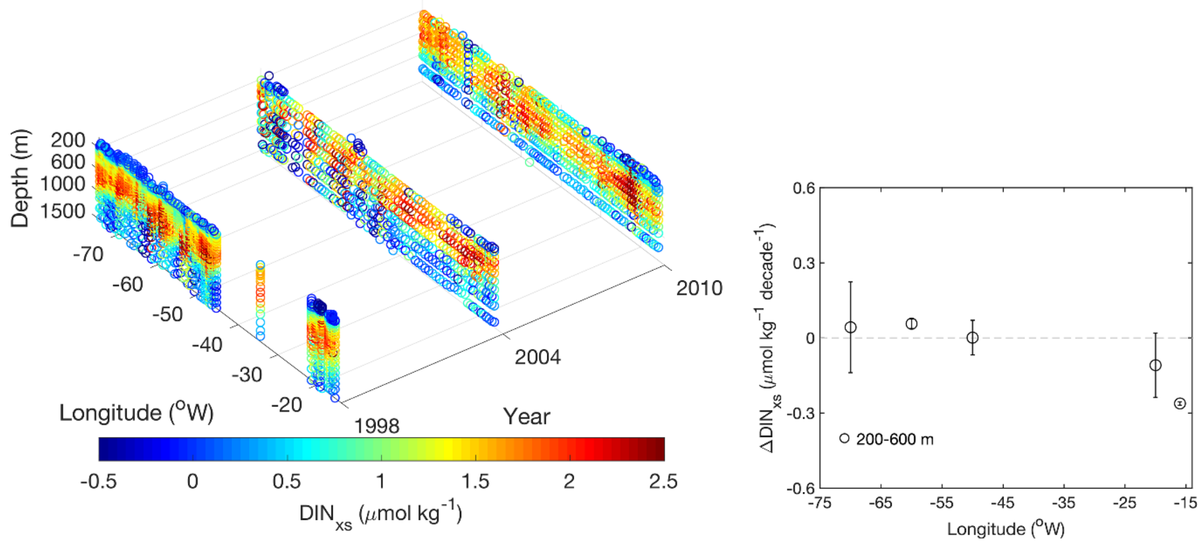

Figure S6. The vertical distributions of excess nitrate (DIN_{xs}) in the upper 1500 m for the difference cruises along the transect A05 in the NAtl. The inset shows the average rates (with 95% confidence limits) of change in DIN_{xs} (ΔDIN_{xs}) at 200–600 m averaged for each 6°–10° longitude interval between GO-SHIP and WOCE time periods.

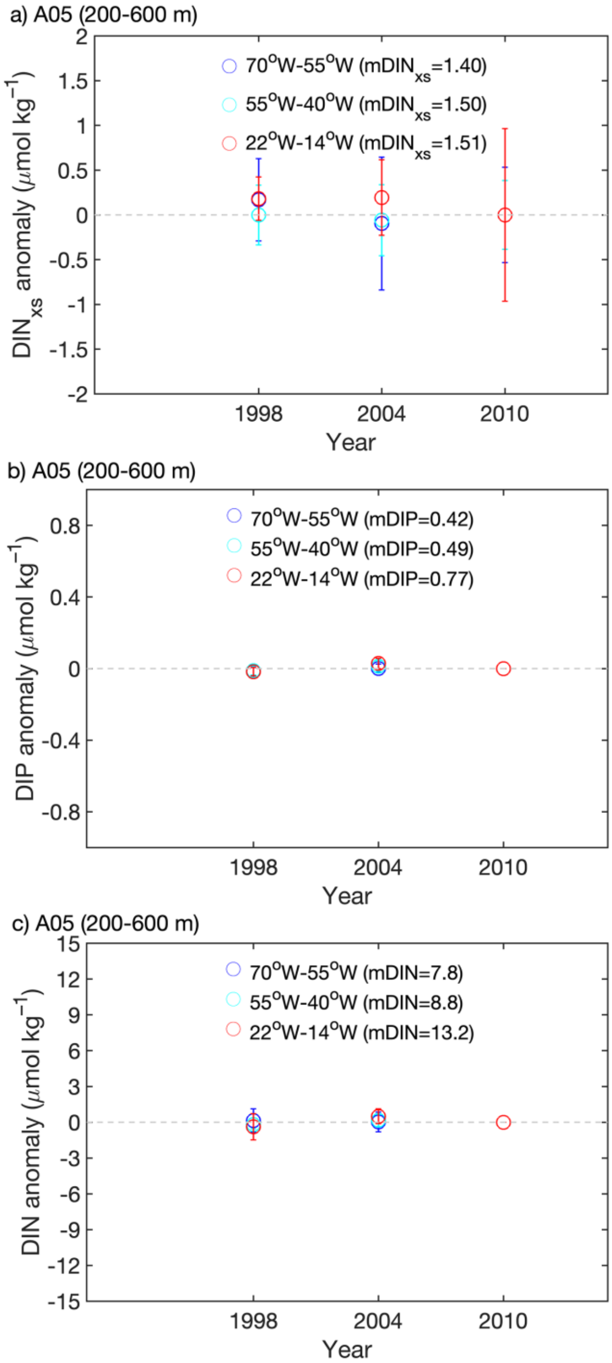

Figure S7. Temporal trends of DIN_{xs} (a), DIP (b) and DIN (c) anomalies for the corresponding longitude intervals for the subsurface potential density intervals σ_θ along A05 (see Fig. S2 caption) in the NAtl. DIN_{xs}, DIP and DIN anomalies indicate DIN_{xs}, DIP and DIN concentrations minus the mean DIN_{xs}, DIP and DIN in GO-SHIP dataset ($mDIN_{xs}$, mDIP and mDIN, their values in parentheses), respectively. The DIN_{xs}, DIP and DIN values were corrected by the changes in AOU (see text). The gray dashed lines in (a) and (b) indicate the DIN_{xs}, DIP and DIN anomalies of zero.

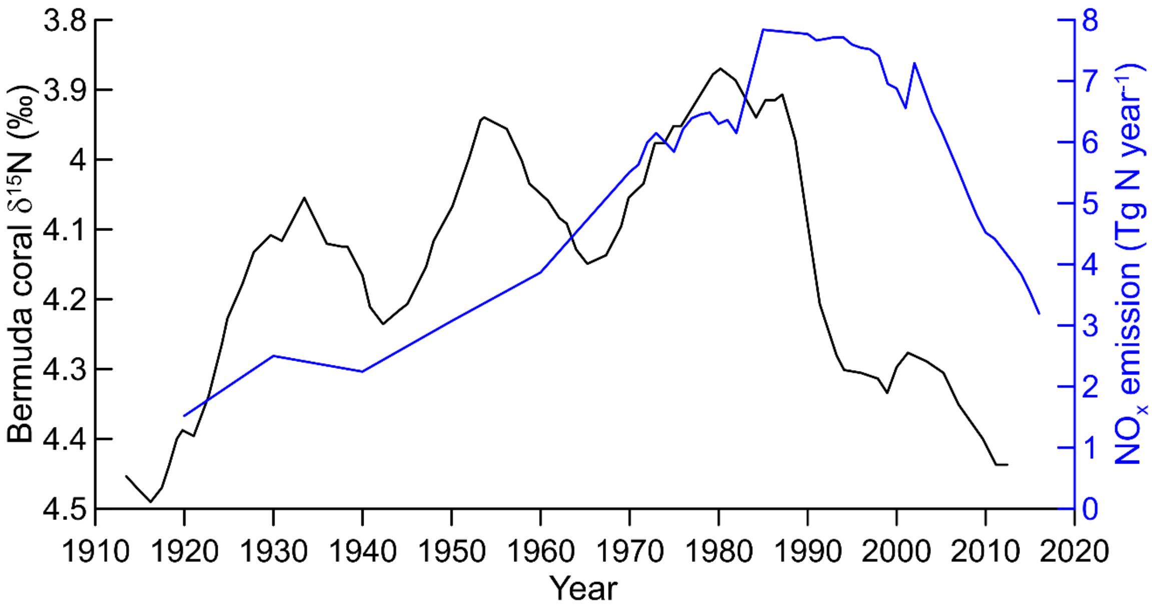

Figure S8. Temporal variations of Bermuda coral $\delta^{15}N$ (black; Wang et al., 2018) and NO_x emissions from the USA (blue; EPA, 2000).

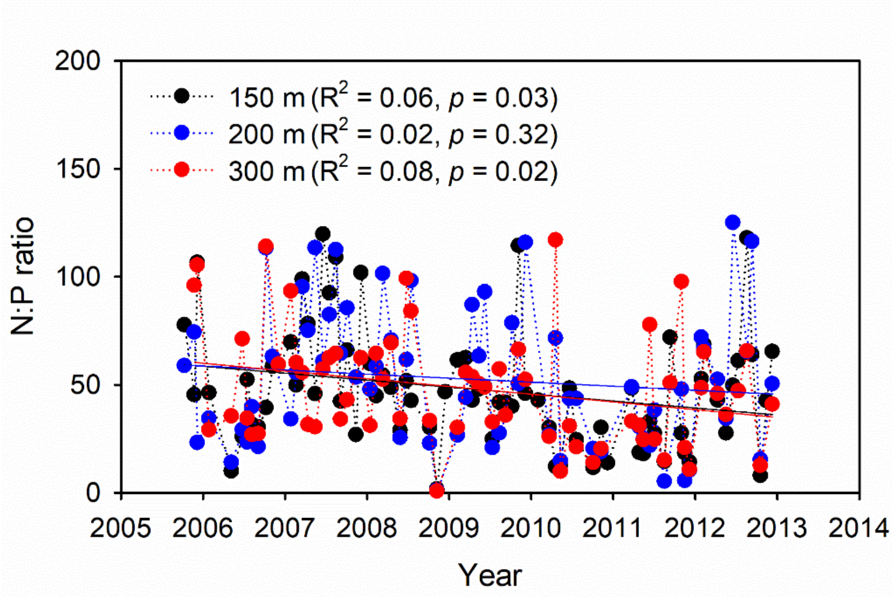

Figure S9. Temporal variations in the N:P ratios in sinking particles collected between 150 and 300 m at the BATS site.

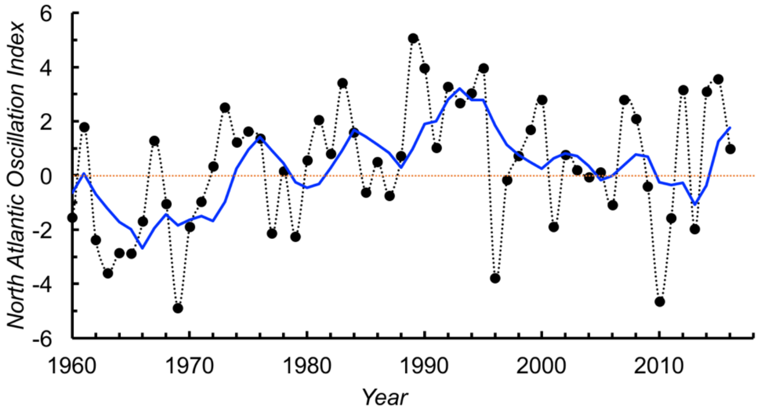

Figure S10. Temporal variation of the winter North Atlantic Oscillation index (solid dots). The blue curve shows the trend of 5-year moving average. Data are derived from the Climate and Global Dynamics division at National Centre for Atmospheric Research (http://www.cgd.ucar.edu/cas/catalog/climind/).

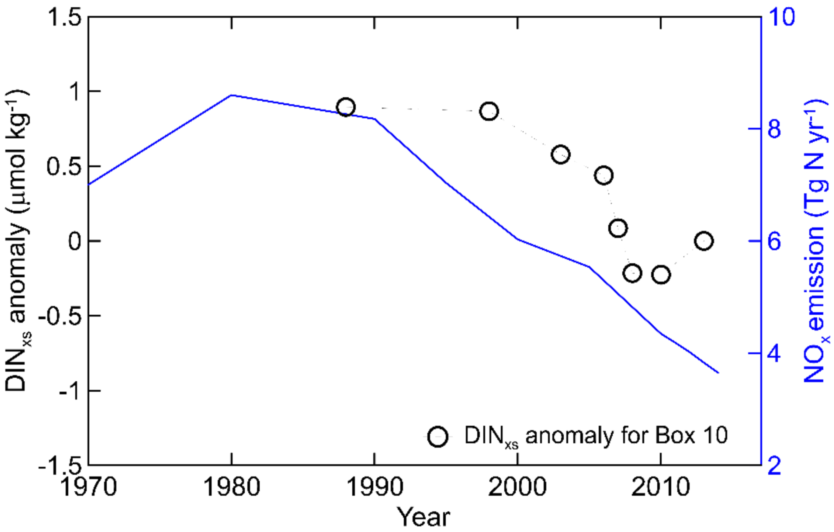

Figure S11. Temporal variations in DIN_{xs} anomaly in the subpolar region of the eastern North Atlantic where DIN_{xs} decreased significantly (box 10 in Figure 5a). The history of NO_x emissions from Europe (blue curve) is also shown (Adams et al., 2012).

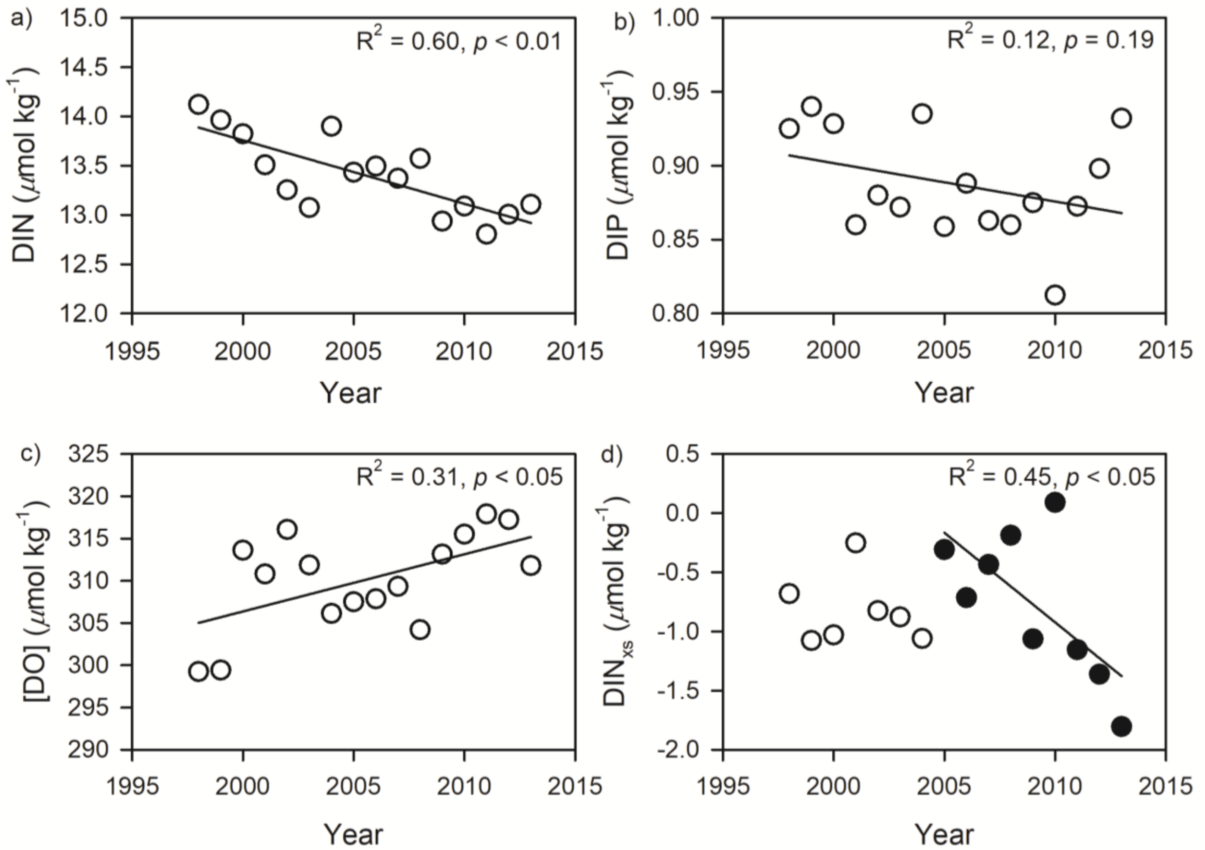

Figure S12. Temporal variations of annual average concentrations of (a) DIN, (b) DIP, (c) dissolved oxygen (DO) and (d) DIN_{xs} in the subsurface waters (300–500 m, potential density σ_θ of ~28.0) at a time series site (68.0°N, 12.7°W) from 1998–2013 in the northern Iceland Sea. Note that the linear regression in d) only include the data since the decreasing trend is significant after 2005. Data are derived from the Ocean Carbon Data System, NOAA (https://www.nodc.noaa.gov/ocads/oceans/Moorings/Iceland_Sea.html).

References

Adams, M., Aardenne, J. V., Kampel, E., Tista, M., and Zuber A.: European Union emission inventory report 1990–2010 under the UNECE Convention on Long-range Transboundary Air Pollution (LRTAP), Eur. Environ. Agency, Copenhagen, http://doi.org/10.2800/5219, 2012.

Anderson, L. A., and Sarmiento, J. L.: Redfield ratios of remineralization determined by nutrient data analysis, Global Biogeochem. Cycles, 8, 65-80, http://doi.org/10.1029/93GB03318, 1994.

Broecker, W. S., and Takahashi, T.: Hydrography of the central Atlantic—III. The North Atlantic deep-water complex, Deep Sea Res. Part A, 27, 591-613, http://doi.org/10.1016/0198-0149(80)90076-X, 1980.

EPA: National Air Pollutant Emission Trends, 1900–1998, Office of Air Quality Planning and Standards, Research Triangle Park, 2000.

Gebbie, G., and Huybers, P.: The mean age of ocean waters inferred from radiocarbon observations: Sensitivity to surface sources and accounting for mixing histories, J. Phys. Oceanogr., 42, 291-305, http://doi.org/10.1175/jpo-d-11-043.1, 2012.

Key, R. M., Olsen, A., van Heuven, S., Lauvset, S. K., Velo, A., Lin, X., Schirnick, C., Kozyr, A., Tanhua, T., Hoppema, M., Jutterström, S., Steinfeldt, R., Jeansson, E., Ishii, M., Perez, F. F., and Suzuki, T.: Global Ocean Data Analysis Project, Version 2 (GLODAPv2), (ORNL/CDIAC-162, ND-P093), Carbon Dioxide Information Analysis Center, Oak Ridge National Laboratory, US Department of Energy, 2015.

Olsen, A., Key, R. M., van Heuven, S., Lauvset, S. K., Velo, A., Lin, X., Schirnick, C., Kozyr, A., Tanhua, T., Hoppema, M., Jutterström, S., Steinfeldt, R., Jeansson, E., Ishii, M., Pérez, F. F., and Suzuki, T.: The Global Ocean Data Analysis Project version 2 (GLODAPv2) – an internally consistent data product for the world ocean, Earth Syst. Sci. Data, 8, 297-323, http://doi.org/10.5194/essd-8-297-2016, 2016.

Talley, L. D., Feely, R. A., Sloyan, B. M., Wanninkhof, R., Baringer, M. O., Bullister, J. L., Carlson, C. A., Doney, S. C., Fine, R. A., Firing, E., Gruber, N., Hansell, D. A., Ishii, M., Johnson, G. C., Katsumata, K., Key, R. M., Kramp, M., Langdon, C., Macdonald, A. M., Mathis, J. T., McDonagh, E. L., Mecking, S., Millero, F. J., Mordy, C. W., Nakano, T., Sabine, C. L., Smethie, W. M., Swift, J. H., Tanhua, T., Thurnherr, A. M., Warner, M. J., and Zhang, J.-Z.: Changes in ocean heat, carbon content, and ventilation: A review of the first decade of GO-SHIP global repeat hydrograpy, Annu. Rev. Mar. Sci., 8, 185-215, http://doi.org/10.1146/annurev-marine-052915-100829, 2016.

Wang, X. T., Cohen, A. L., Luu, V., Ren, H., Su, Z., Haug, G. H., and Sigman, D. M.: Natural forcing of the North Atlantic nitrogen cycle in the Anthropocene, Proc. Natl. Acad. Sci., 115, 10606-10611, http://doi.org/10.1073/pnas.1801049115, 2018.

Woosley, R. J., Millero, F. J., and Wanninkhof, R.: Rapid anthropogenic changes in CO_2 and pH in the Atlantic Ocean: 2003–2014, Global Biogeochem. Cycles, 30, 70-90, http://doi.org/10.1002/2015GB005248, 2016.

Zhang, J.-Z., Mordy, C. W., Gordon, L. I., Ross, A., and Garcia, H. E..: Temporal trends in deep ocean Redfield ratios, Science, 289, 1839-1839, http://doi.org/10.1126/science.289.5486.1839a, 2000.